Electronic Supplementary Material (ESI) for Journal of Materials Chemistry A.

Adjacent atomic cobalt sites anchored on carbon foam as self-supporting electrode for efficient hydrogen evolution

Yingxue Wang[a], Jing Yu[a*], Jiahui Zhu[a*], Qi Liu[a], Jingyuan Liu[a], Rongrong Chen[a], Rumin Li[a], Jun Wang[a]

a Key Laboratory of Superlight Materials and Surface Technology, Ministry of Education, College of Materials Science and Chemical Engineering, Harbin Engineering University, 150001, China

E-mail: jing.yu@hrbeu.edu.cn, zhujiahui@hrbeu.edu.cn

Electrochemical measurements

All electrochemical tests were carried out on an electrochemical workstation (CHI 760E) using a three-electrode system. Platinum sheet was employed as the counter electrode, Ag/AgCl (0.5 M H_2SO_4) or Hg/HgO (1 M KOH) was used as the reference electrode, and the self-supporting carbon foam loaded cobalt single atoms were used as the working electrode (1 cm × 0.5 cm). The HER performance tests were performed in 1 M KOH and 0.5 M H_2SO_4 in three-electrode system. The overpotential was determined by measuring the linear sweep voltammetry (LSV). All potentials were calibrated by reversible hydrogen electrode and compensated by *iR*. Electrochemical impedance spectroscopy (EIS) was measured at 5 mV AC voltage in the frequency range of 10^5 Hz ~ 10^{-1} Hz. Cyclic voltammetry (CV) was used to measure the curves at different scanning rates (60, 100, 140, 180, 220, 260 mV s^{-1}) to calculate the electric double layer capacitance (C_{dl}). The stability test was carried out by accelerated cyclic voltammetry (2000 CV cycles). Turnover frequency (TOF) was calculated by assuming all Co single atoms participating in the reaction according to the equation: TOF = $JA/2nF$, where J is the current density, A is the electrode geometric area, 2 represents 2 electrons for H_2 per mol, n is the mole number of active sites, and F is the Faraday constant of 96485.3 C mol^{-1}.

Computational method

All calculations were performed using the Vienna Ab-initio Simulation Package (VASP). The Perdew-Burke-Ernzerhof (PBE) functional for the exchange correlation term was used with the projector augmented wave (PAW) potentials and a cutoff energy

of 400 eV. A 2×2×1 Monkhorst-Pack K-point and spin polarization were set in this calculation. The vacuum layer was set as 15 Å to avoid the interactions between layers. The convergence of energy and forces were set to 1×10^{-5} eV and 0.02 eV/Å, respectively. The adsorption energy (ΔE_{ad}) was calculated as: $\Delta E_{ad} = E_{(surf + ad)} - E_{(surf)} - E_{(ad)}$, where $E_{(surf + ad)}$, $E_{(surf)}$, and $E_{(ad)}$ are the energies of the H_2O molecule adsorbed on the surface of the isolated Co or Co_1/Co_2, surface of the isolated Co or Co_1/Co_2 and the H_2O molecule, respectively. The HER calculation was adopted "Computational Hydrogen Electrode" (CHE) model, and the reaction was $H^+ + e^- = 1/2\ H_2$. The free energies of the HER intermediate were obtained by $\Delta G = \Delta E + \Delta ZPE - T\Delta S$, where ΔE, ΔZPE and ΔS are the binding energy, zero point energy change and entropy change, respectively. The ΔZPE and ΔS were obtained according to the NIST or calculated by the VASPKIT program.

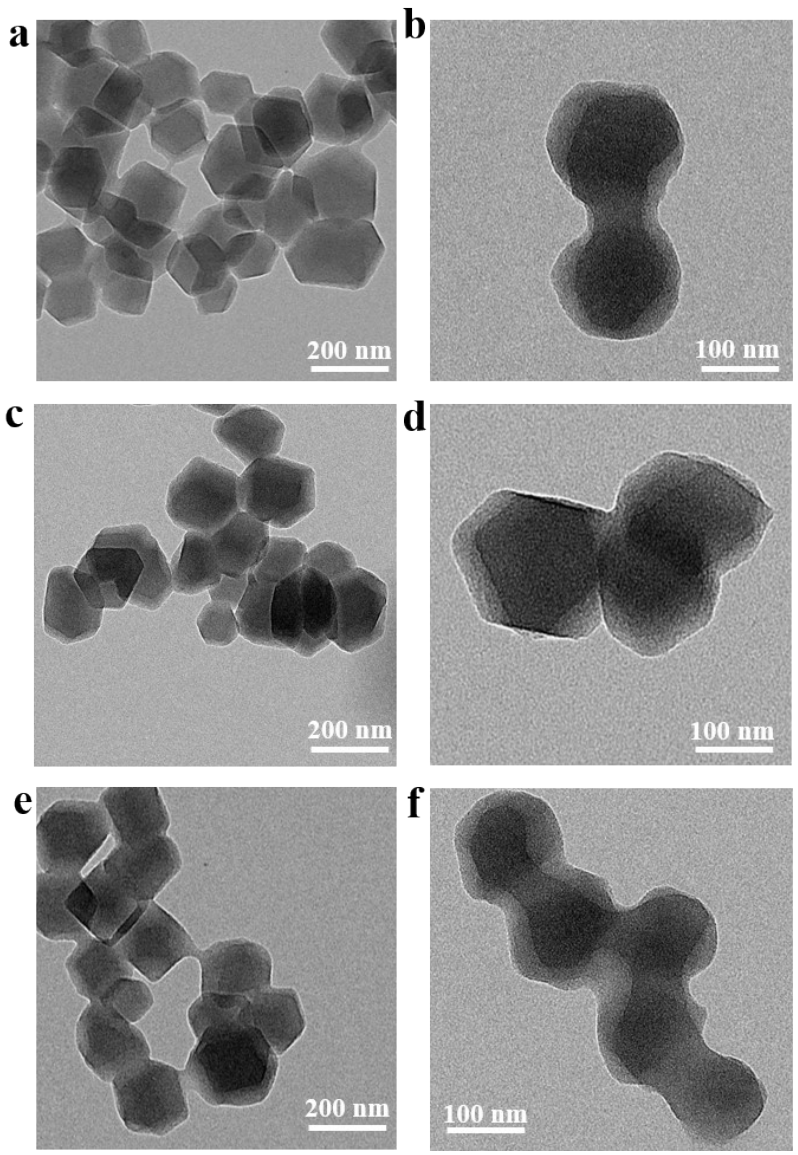

Fig. S1. TEM images of (a, b) $Zn_{10}Co_1$-MOF, (c, d) $Zn_{15}Co_1$-MOF and (e, f) $Zn_{20}Co_1$-MOF.

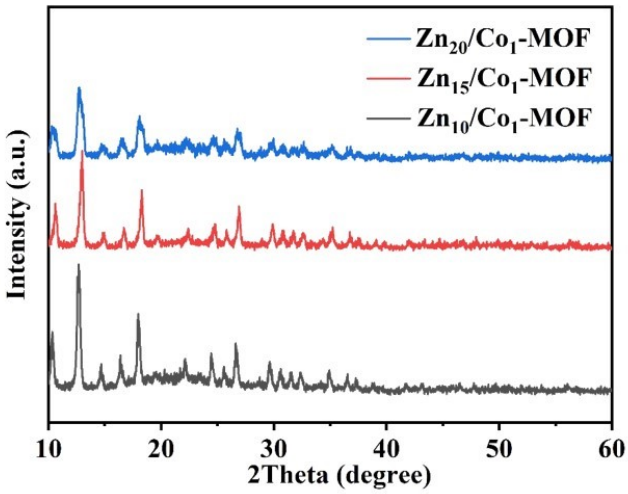

Fig. S2. XRD patterns of $Zn_{10}Co_1$-MOF, $Zn_{15}Co_1$-MOF and $Zn_{20}Co_1$-MOF.

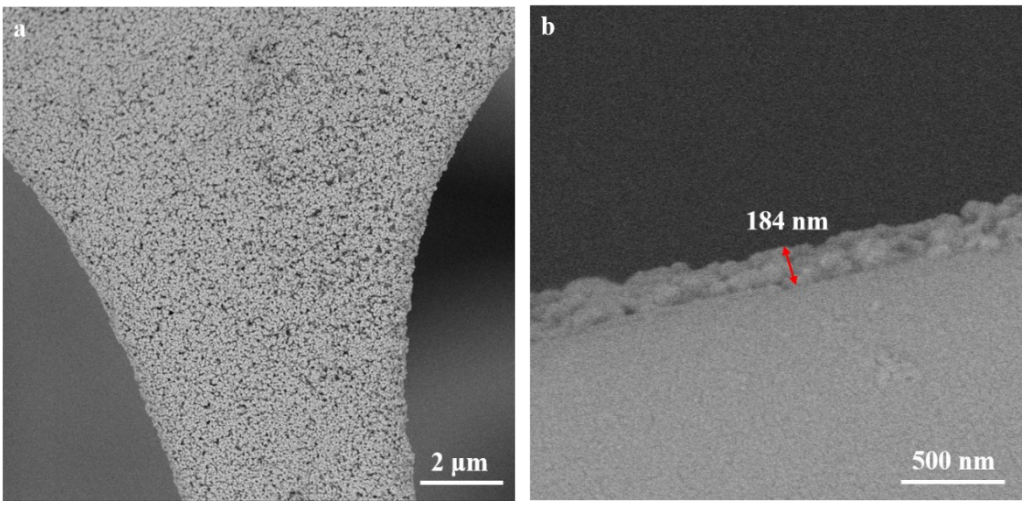

Fig. S3. (a) SEM image of $Zn_{20}Co_1$-MOF/MF, (b) cross-section SEM image of $Zn_{20}Co_1$-MOF/MF.

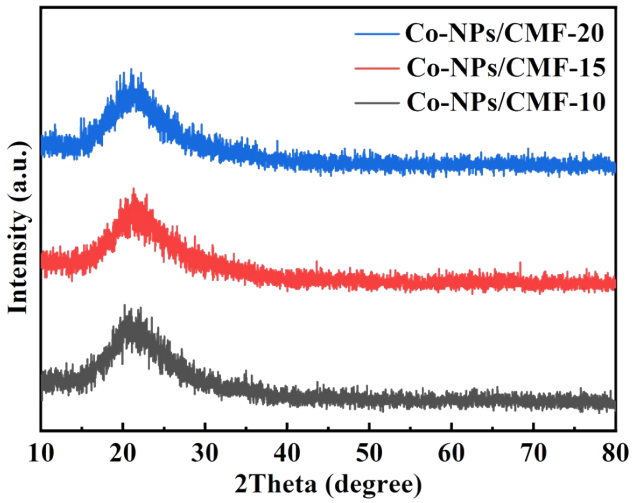

Fig. S4. XRD patterns of Co-NPs/CMF-10, Co-NPs/CMF-15 and Co-NPs/CMF-20.

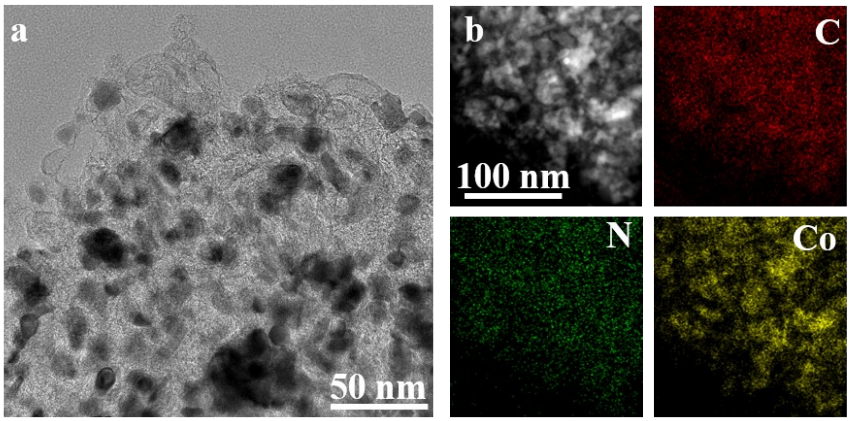

Fig. S5. (a) Co-NPs/CMF-20, (b) EDS element mappings of Co-NPs/CMF-20.

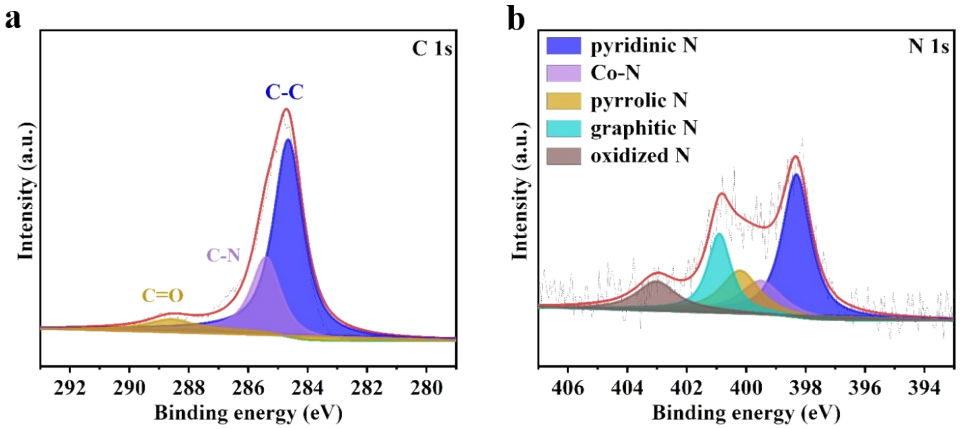

Fig. S6. (a) C 1s and (b) N 1s XPS spectra of Co-NPs/CMF-20.

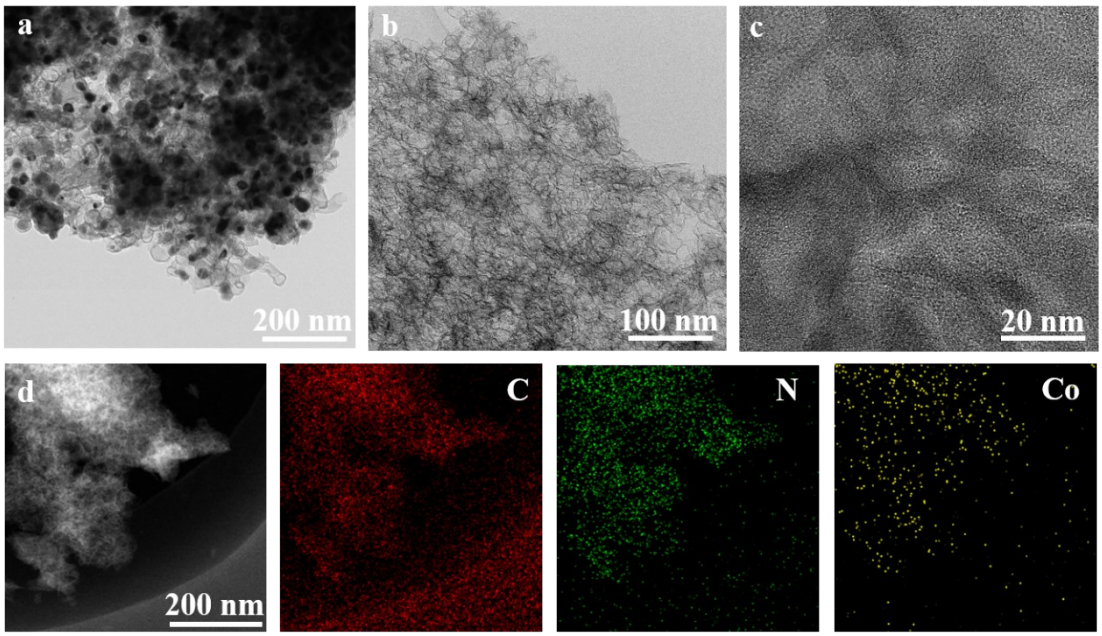

Fig. S7. TEM images of (a) Co-NPs/CMF-10 and (b) Co-N/CMF-10. (c) HRTEM image of Co-N/CMF-10. (d) EDS element mappings of Co-N/CMF-10.

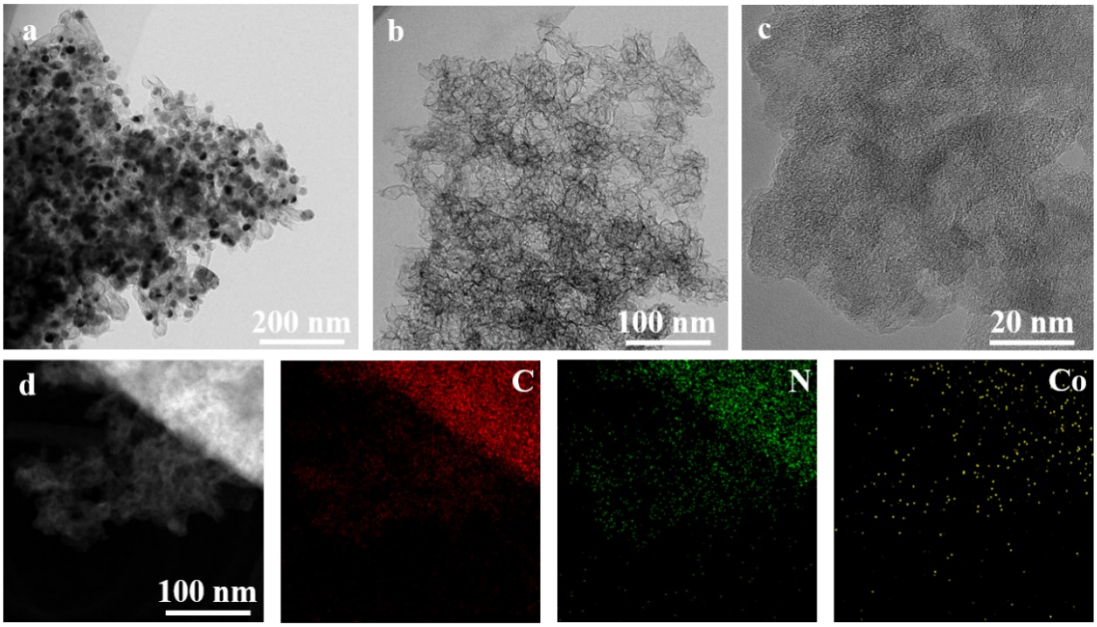

Fig. S8. TEM images of (a) Co-NPs/CMF-15 and (b) Co-N/CMF-15. (c) HRTEM image of Co-N/CMF-15. (d) EDS element mappings of Co-N/CMF-15.

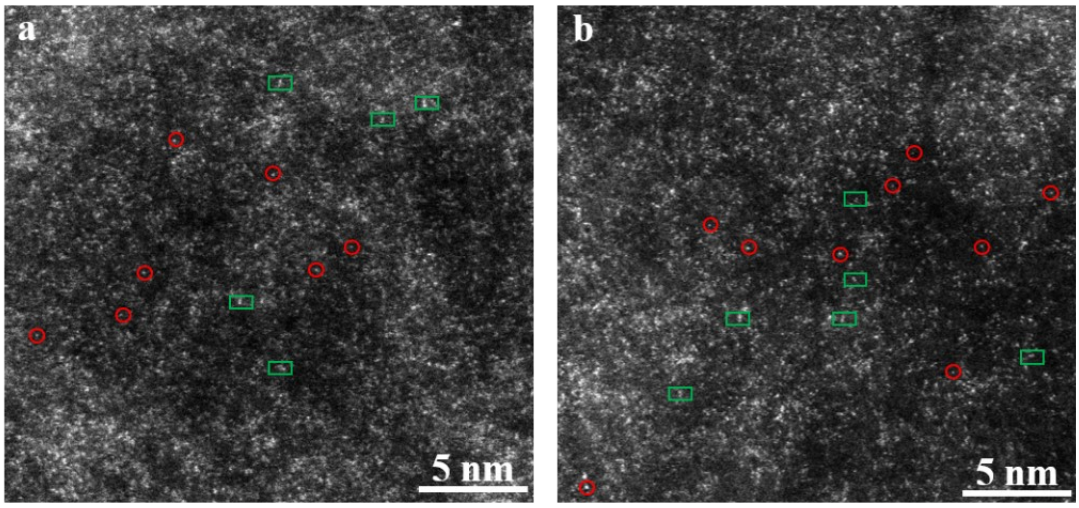

Fig. S9. (a, b) AC-HAADF-STEM images of Co-N/CMF-20.

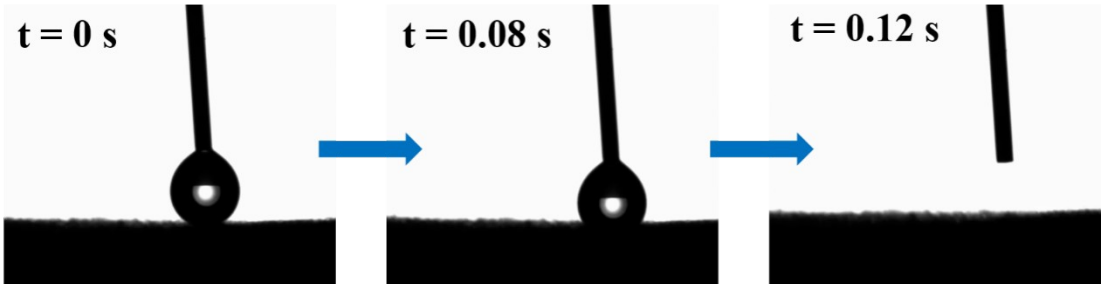

Fig. S10. Contact angle analysis of Co-N/CMF-20.

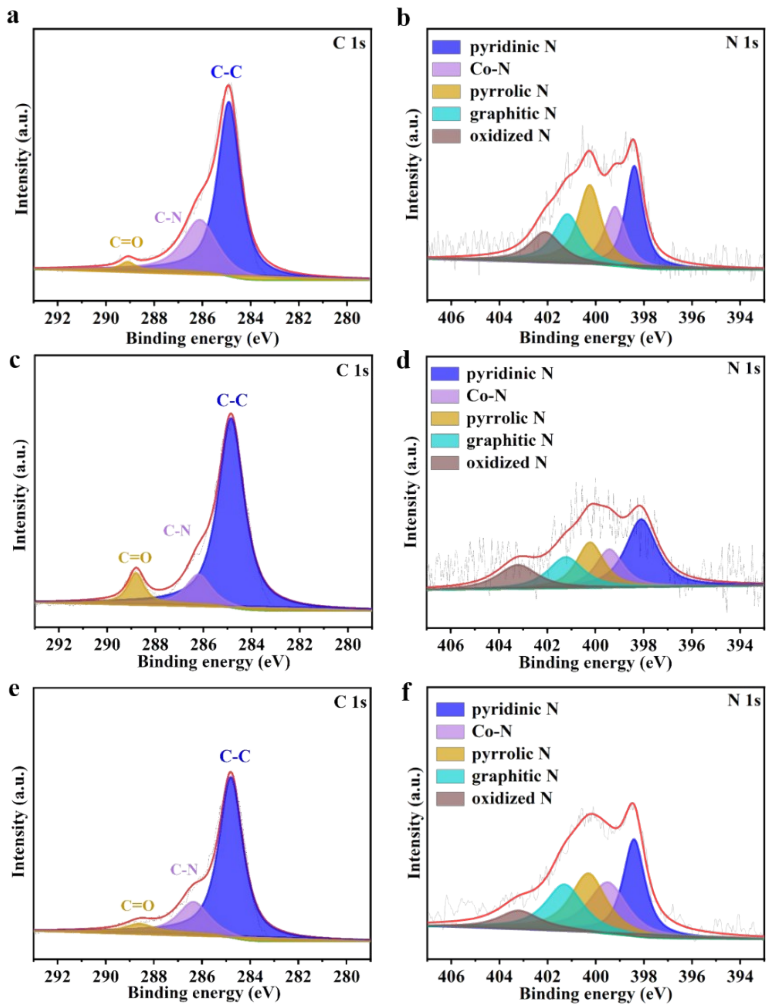

Fig. S11. XPS spectra of (a) C 1s and (b) N 1s of Co-N/CMF-10. XPS spectra of (c) C 1s and (d) N 1s of Co-N/CMF-15. XPS spectra of (e) C 1s and (f) N 1s of Co-N/CMF-20.

Table S1. Comparison of HER performances of Co-N/CMF-20 with reported single atom electrocatalysts in 0.5 M H_2SO_4.

Electrocatalysts	η_{10} (mV)	Reference
Co-N/CMF-20	41.3	This work
Co-I-N/G	52	ACS Nano 2021 15, 18125-18134.
Co-NMGO	146	Adv. Energy Mater. 2021,11, 2101619.
Ru-MoS_2/CC	61	Appl. Catal. B 2019,249,91-97.
CoN_3-CSG	82	Small 2022, 18, 2201139.
Pt/TiO_{2-X}	95	Mater. Today Energy 2021, 22, 100877.
$Ru_{0.10}$@2H-MoS_2	168	Appl. Catal. B 2021, 298, 120490.
NCAG/Ru-3	65	Chem. Eng. J. 2022, 442, 136337.
MoS_2/(CoNi@G)	150	Nano Energy 2020, 72, 104700.
Co SA-Co NPs/NCFs	106	J. Energy Chem. 2022, 67, 147-156.
Co−NC−AF	87	Adv. Mater. 2021, 33, 2103533.
MoS_2-60s	131	J. Am. Chem. Soc. 2020, 142, 4298-4308.
Pt/TiBxOy	50	ACS Catal. 2022, 12, 5970-5978.
Rh@NG	29	Carbon 2020, 164, 121-128.
Rh-MoS_2-4.8	67	Angew. Chem. 2020, 132, 10588-10593.
$Pt_{0.47}$-Ru/Acet	28	Chem. Eng. J. 2022, 448, 137611.
Co-doped WO_3/CF	117	ACS Appl. Mater. Interfaces 2021, 13, 45, 53915-53924.
Mo SAs@1T-CrS_2	97	Chem. Eng. J. 2022, 428, 131210.
Co_4N@CoSA/N-CNT/CC	78	NPG Asia Mater. 2021, 13:1.
g-C_3N_4-C-TiO_2	112	ACS Appl. Mater. Interfaces 2021, 13, 39, 46608-46619.
MoS_2/CoSAs-NS-CNTs@CoS_2/CC	72	Appl. Catal. B 2021, 298, 120630.

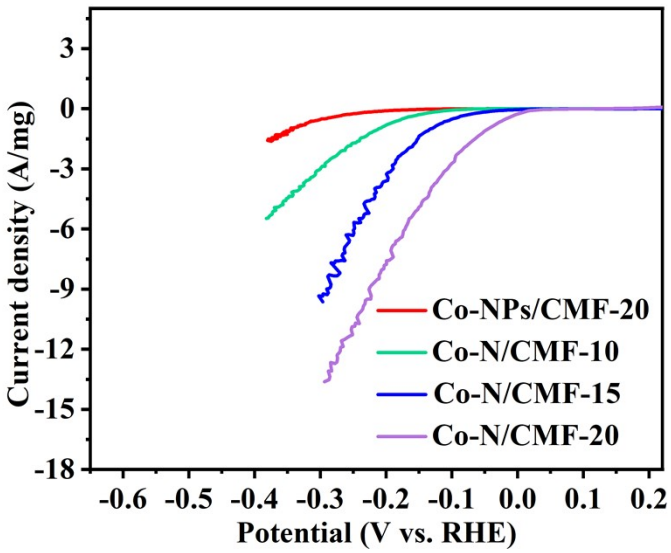

Fig. S12. The mass activities for HER in 0.5 M H_2SO_4.

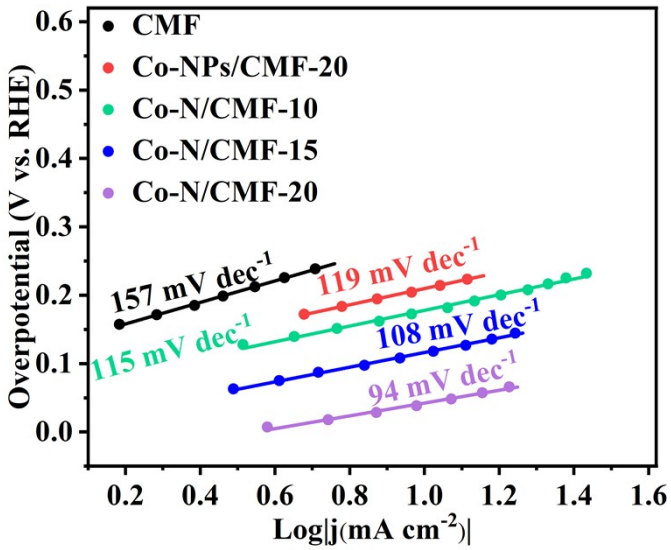

Fig. S13. Corresponding Tafel plots for HER in 0.5 M H_2SO_4

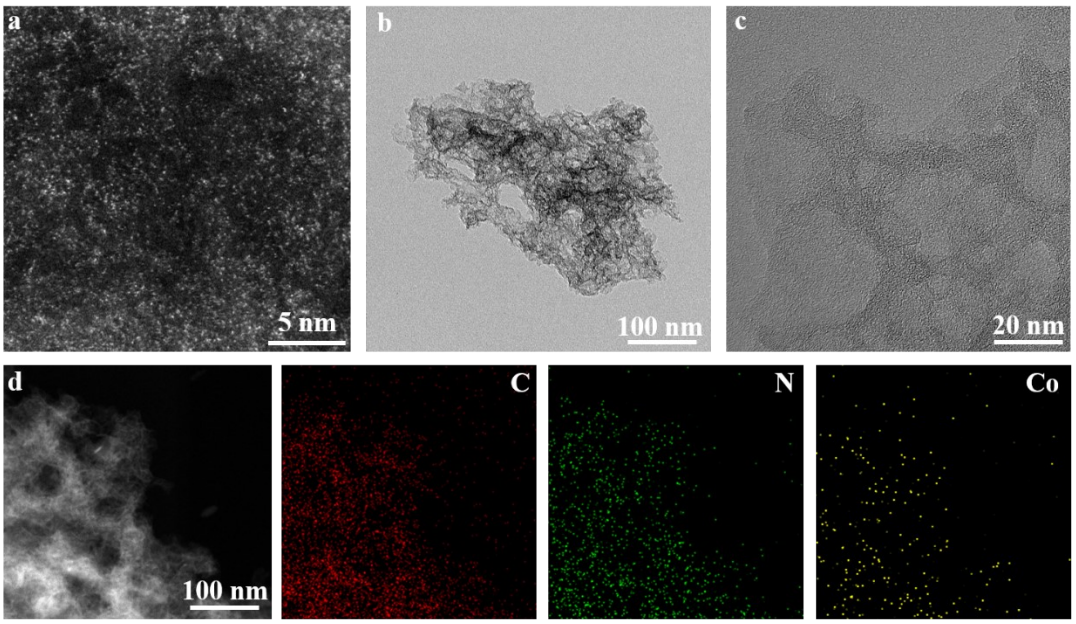

Fig. S14. Structural characterization of Co-N/CMF-20 after HER Test in 0.5 M H_2SO_4 (a) AC-HAADF-STEM images, (b) TEM, (c) High-magnification TEM image, (d) EDS element mappings.

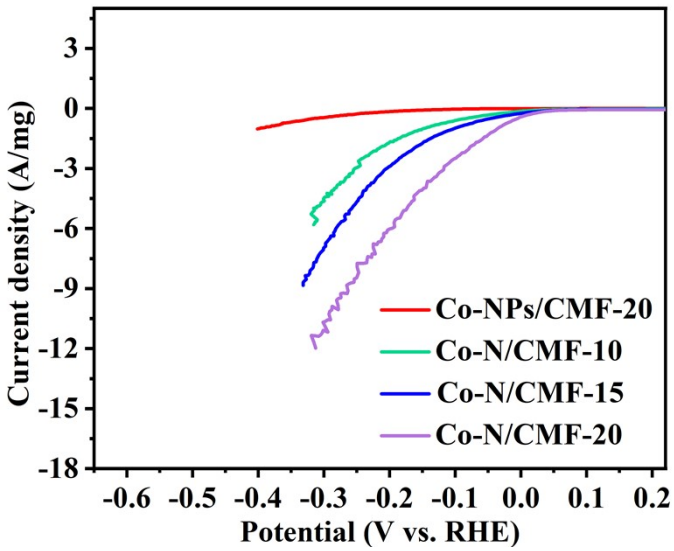

Fig. S15. The mass activities for HER in 1 M KOH.

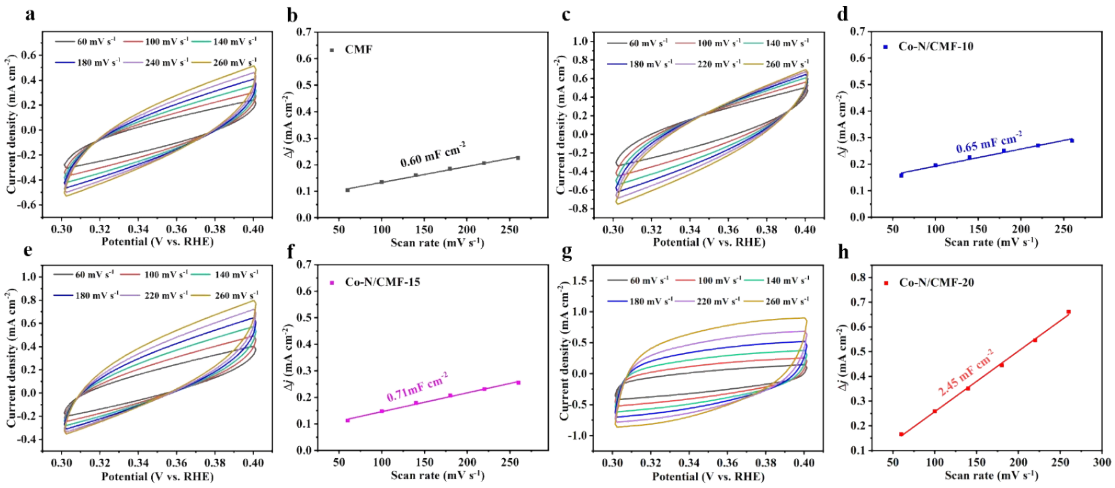

Fig. S16. Cyclic voltammetry (CV) curves of (a) CMF, (c) Co-N/CMF-10, (e) Co-N/CMF-15, (g) Co-N/CMF-20. (b, d, f, h) Capacitive current as a function of scan rate.

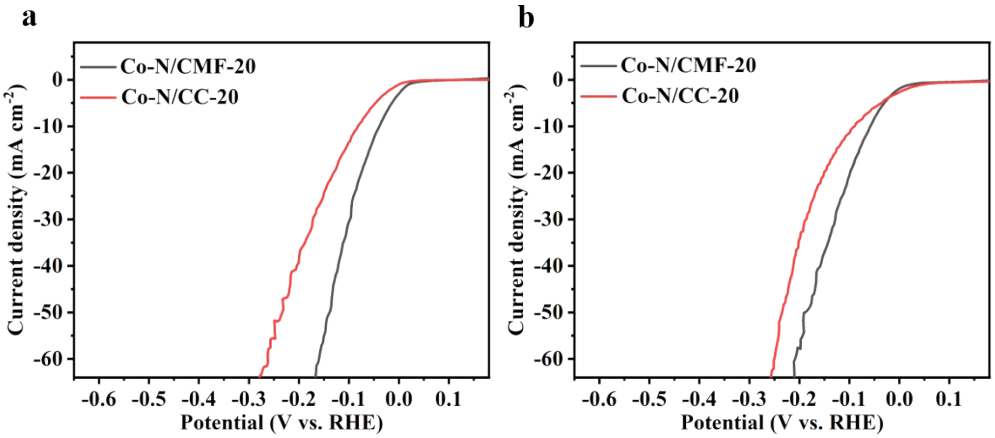

Fig. S17. Electrocatalytic measurements of Co-N/CMF-20 and Co-N/CC-20 (a) HER LSV polarization curves in 0.5 M H_2SO_4, (b) HER LSV polarization curves in 1 M KOH.

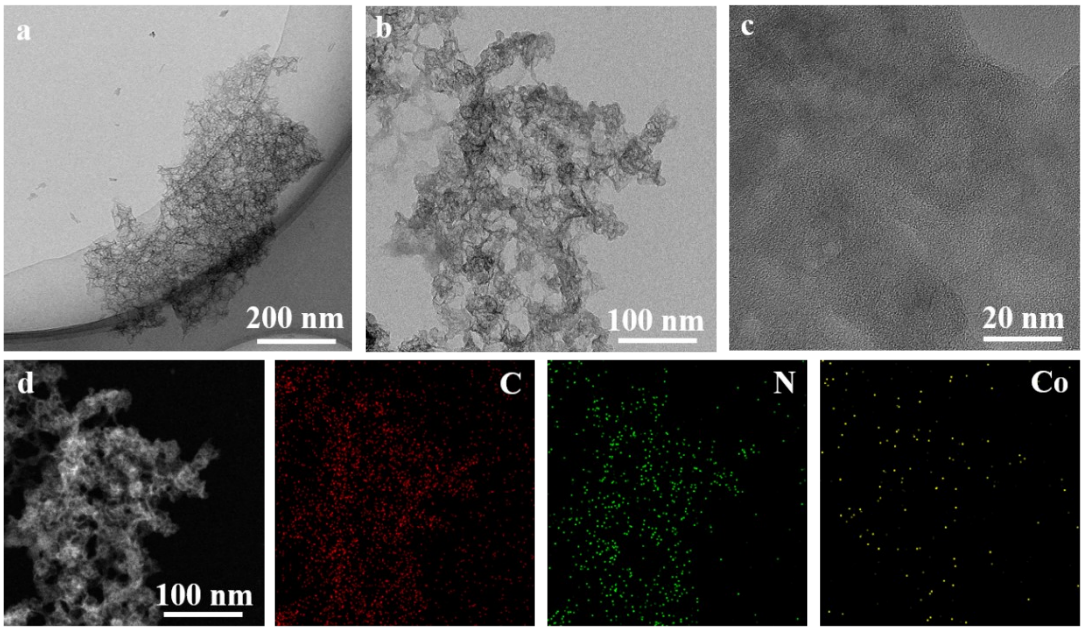

Fig. S18. (a, b) TEM images of Co-N/CMF-20, (c) high-magnification TEM image of Co-N/CMF-20, (d) EDS element mappings of Co-N/CMF-20 after HER test in 1 M KOH.

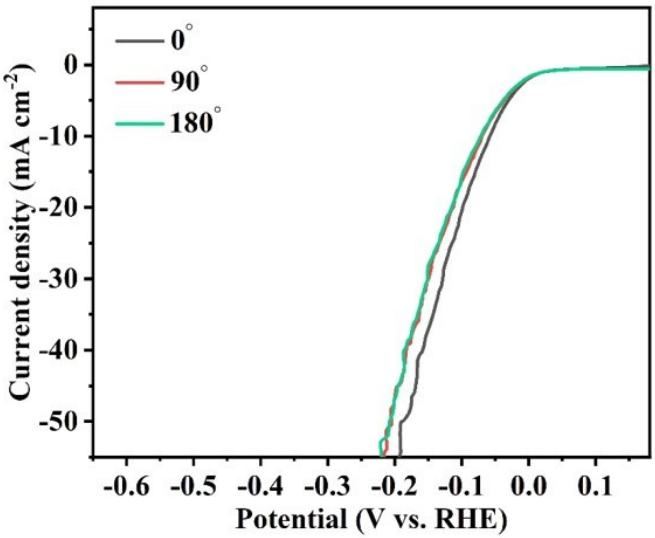

Fig. S19. The LSV curves of Co-N/CMF-20 at bending angles of 0, 90, and 180 ° for HER in 1 M KOH.

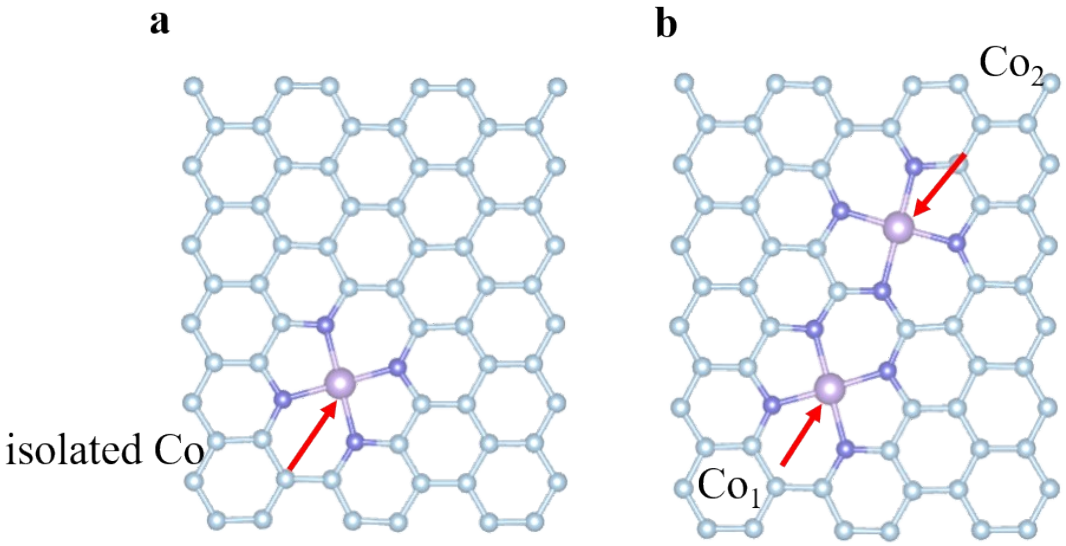

Fig. S20. Atomic models of simulated (a) isolated Co and (b) adjacent Co atoms.

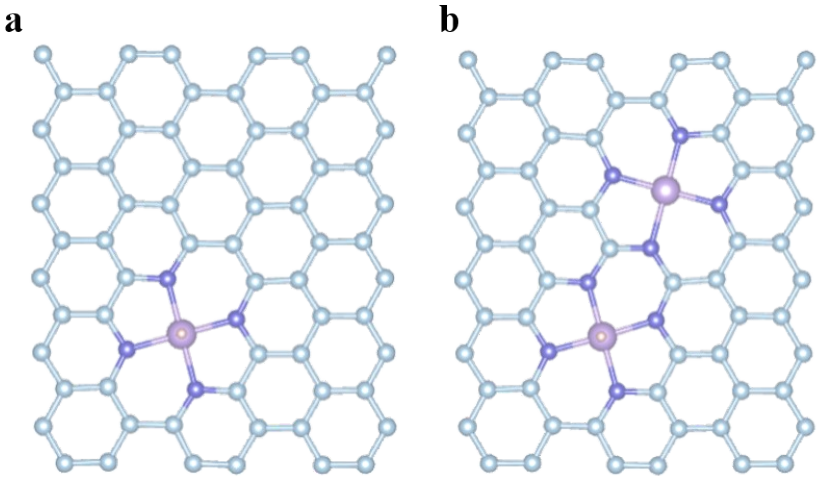

Fig. S21. Calculated H adsorption for HER on (a) isolated Co and (b) adjacent Co atoms.